




**Two-dimensional electromagnetically induced phase grating via composite vortex light**Seyyed Hossein Asadpour <sup>1</sup>, Hamid R. Hamed, <sup>2</sup> Teodora Kirova <sup>3,\*</sup> and Emmanuel Paspalakis <sup>4</sup><sup>1</sup>*Department of Physics, Iran University of Science and Technology, Tehran 1684613114, Iran*<sup>2</sup>*Institute of Theoretical Physics and Astronomy, Vilnius University, LT-10257, Lithuania*<sup>3</sup>*Institute of Atomic Physics and Spectroscopy, University of Latvia, LV-1004, Latvia*<sup>4</sup>*Materials Science Department, School of Natural Sciences, University of Patras, Patras 265 04, Greece*

(Received 29 September 2021; revised 22 February 2022; accepted 22 March 2022; published 8 April 2022)

We investigate the performance of a symmetrical two-dimensional electromagnetically induced grating produced in a four-level  $N$ -type atomic scheme, which interacts with a weak probe field and two simultaneous coupling fields: a two-dimensional standing wave and a composite optical vortex beam. Based on the Maxwell wave equation, we study numerically the behavior of the amplitude, the phase modulations, as well as the probe field diffraction intensities of different order under various conditions for the coupling field detunings and the orbital angular momentum of the Laguerre-Gaussian field. The different orders of diffraction are altered when the azimuthal angle of the composite vortex light changes, thus producing a two-dimensional symmetric grating which transfers the probe energy to higher orders of diffraction. A detailed analysis of the probe field energy transfer to these different orders proves the possibility for direct control over the performance of the grating.

DOI: [10.1103/PhysRevA.105.043709](https://doi.org/10.1103/PhysRevA.105.043709)**I. INTRODUCTION**

Electromagnetically induced transparency (EIT) [1,2] lies at the foundation of many novel phenomena in quantum optics. It utilizes quantum interference of double optical transitions, which causes the vanishing of a weak probe field absorption under the action of a strong coupling field. EIT is well developed both theoretically and experimentally with many applications in different fields, such as slow or stopped light and light storage [3–5], quantum information [6,7], and nonlinear optics [8,9]. Upon applying a standing-wave (SW) coupling field in the EIT system, the absorption and dispersion of the traveling wave (TW) probe field become spatially periodic, leading to the so-called electromagnetically induced grating (EIG) [10–12]. Since EIGs give opportunities for manipulating the amplitude and phase modulations of the weak probe beam, as well as the intensity distribution of the different grating orders, they open novel applications in optical switching [13], storing propagated light through an atomic medium [14], and all-optical beam splitting and fanning [15].

The original EIG  $\Lambda$  scheme has been further extended to V systems in cold atoms [16] and  $\Xi$ -type excitations [17]. Of particular interest for the present work are the more complicated four-level configurations, involving interactions with multiple fields:  $Y$  type [18], tripod atomic systems [19], and others [20], including interesting processes happening near plasmonic nanostructures [21] and in quantum wells [22].

Other exotic examples of EIG applications are electromagnetically induced Talbot effect [23], improving the structure of photonic band gaps [24], optical bistabilities [25],

multicomponent vector solitons [26], and two-dimensional surface solitons [27].

Usually the formed gratings diffract light symmetrically; however, in the  $\mathcal{PT}$ -symmetric media it is also possible to observe asymmetric diffraction patterns due to the spatially modulated refractive index of the light [28–30].

The interaction of atoms with optical vortex beams, e.g., light beams carrying orbital angular momentum (OAM) [31] provides additional degrees of freedom in manipulating the optical properties of the media. The latter leads to new applications in optical technologies, communication [32,33], and quantum information [34]. Schemes involving optical vortices have been recently extended to spatially dependent EIT [35,36], vortex slow light [37,38], exchange of OAM modes in multilevel quantum systems [39,40], as well as semiconductor quantum-dot molecules and quantum wells [41,42]. Vortex beams have also found interesting uses in creating chiral nanostructures [43], three-dimensional optical trapping of metallic nanoparticles [44], and optical tweezers [45].

Specifically, composite optical vortices are formed when two or more beams interfere [46,47]. By using pairs of Laguerre-Gauss modes with different vortex indices a Ferris wheel for ultracold atoms can be implemented [48,49], generating bright ring lattices for trapping atoms in red-detuned light and dark ring lattices for trapping atoms in blue-detuned light. Such optical ring lattices have self-healing properties [50] and give rise to the creation of artificial gauge magnetic and electric fields [51].

In addition, the continuous azimuthal deformation of vortex solitons leads to a novel class of spatially localized self-trapped ringlike singular optical beams called azimuthons [52,53].

Motivated by the ability of the light OAM to provide additional degrees of freedom to various control schemes, as well

\*teo@lu.lv

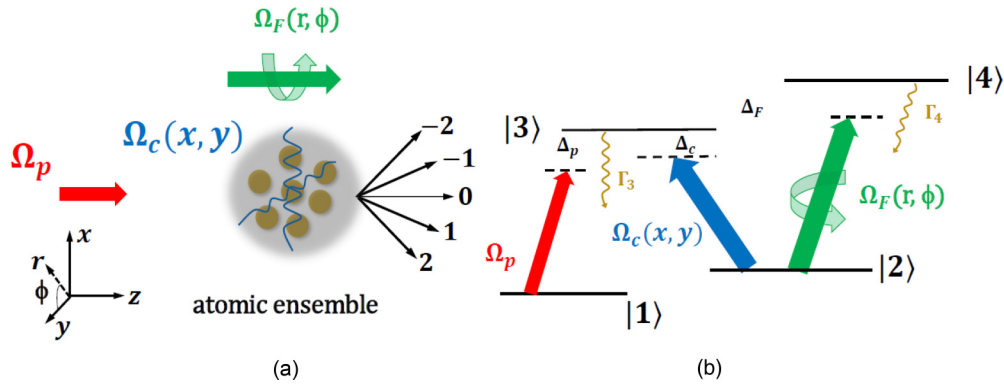


FIG. 1. (a) Excitation scheme of atomic ensemble in EIG. Atoms are excited by a weak TW probe field with Rabi frequency  $\Omega_p$  and two simultaneous coupling fields: a SW with Rabi frequency  $\Omega_c$  and an optical vortex with Rabi frequency  $\Omega_F$ . (b) Atomic  $N$ -type configuration. More details are given in the text.

as the increased possibilities that multilevel systems can give, we study the effects of the interaction of an atomic  $N$ -level EIG scheme with a composite light vortex, expecting such an application to give rise to novel phenomena for manipulating the EIG performance. To this end, in this work we propose a theoretical scheme for the realization of a controllable symmetric EIG based on the simultaneous use of two spatially dependent coupling fields: a two-dimensional SW and composite laser beam carrying OAM in an  $N$ -level atomic configuration. We distinguish between two specific cases, e.g., when all applied fields are resonant with their corresponding atomic transitions, and when the composite vortex light is off-resonant, while the probe field remains on resonance. Our numerical studies show that while in the first case only an amplitude grating can be achieved, in the second one both the amplitude and the phase modulations of the probe light become nonzero. At the same time, changing the azimuthal index of the composite Laguerre-Gaussian field can serve as a control knob for the distribution of the probe field energy into high orders of diffraction. Due to this easy achievable controllability, we expect the proposed EIG scheme to be also experimentally feasible in a typical EIG setup [11,12], with

foreseen application in EIT-based quantum devices, information manipulation, and processing.

It is worth noting that, in most previous studies the main part of the probe energy remains in the zero order of diffraction and only some of the probe energy transfers to the high orders of diffractions. However, in the case of phase grating due to adjusting the phase modulation of the transmitted light, most of the probe energy transfers to the high orders and only a small portion of the energy gathers in the zero order. In previous works different mechanisms have been proposed for transferring the probe energy from zero order to high orders, such as spontaneously generated coherence (SGC) or relative phase between the applied lights. The strengths of our proposed model lays in the fact that we suggest an alternative interesting and easy way for adjusting the phase grating mechanism via composite vortex light, where the probe energy can be transferred from zero order to high orders by adjusting the OAM number and the azimuthal angle of the composite vortex light.

The paper is organized as follows. Section II is devoted to the theoretical model, serving as a base for our numerical calculations, including Maxwell's equation in the slowly varying envelope approximation and the Fraunhofer diffraction

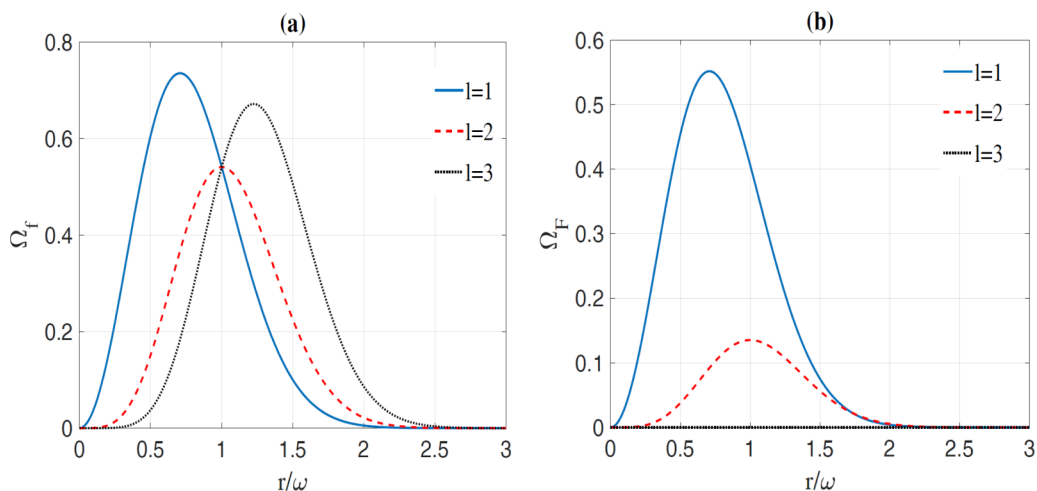


FIG. 2. The Rabi frequencies  $\Omega_f$  and  $\Omega_F$  versus  $r/w$  for different values of the parameter  $l$ . Other selected parameters are  $\Phi = \pi/6$  and  $\Omega = \gamma$ .

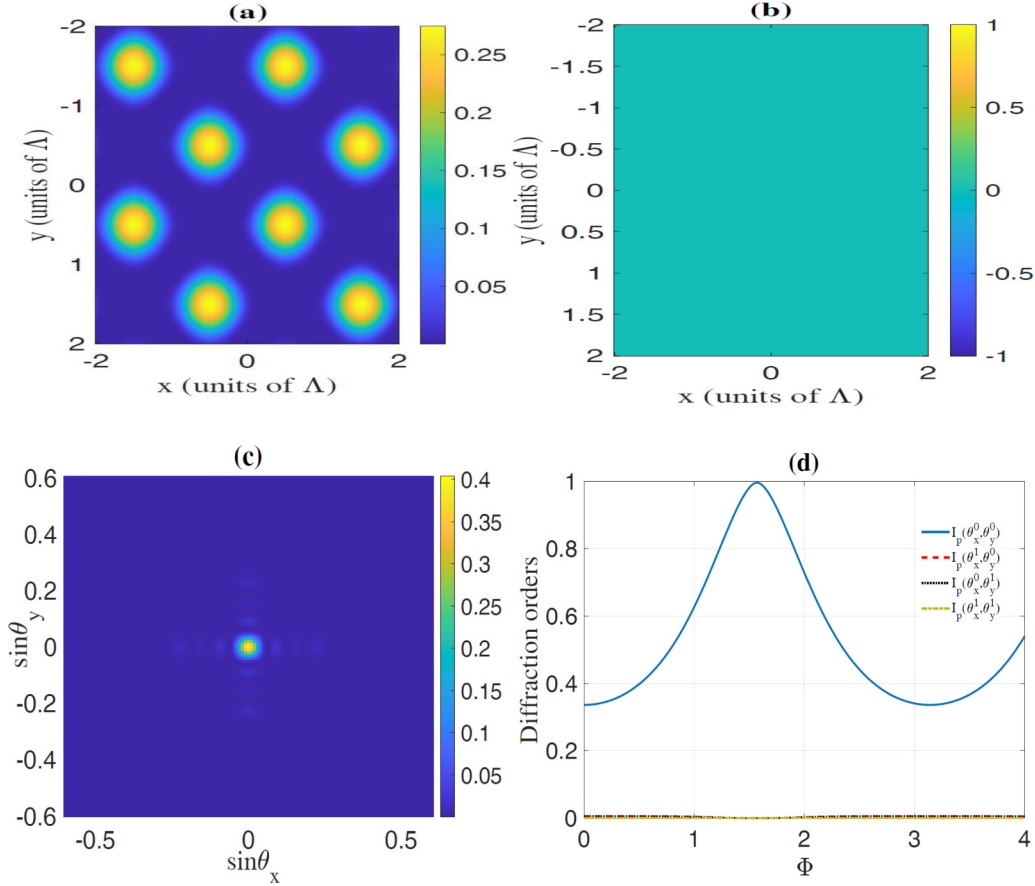


FIG. 3. Amplitude (a) and phase (b) modulations of probe light as a function of  $x$ ,  $y$ , and diffraction pattern (c) as a function of  $\sin\theta_x$  and  $\sin\theta_y$ . (d) The diffraction intensities  $I_p(\theta_x^0, \theta_y^0)$ ,  $I_p(\theta_x^1, \theta_y^0)$ ,  $I_p(\theta_x^0, \theta_y^1)$ , and  $I_p(\theta_x^1, \theta_y^1)$  as a function of the phase  $\Phi$ . The selected parameters are  $\Delta_p = \Delta_c = \Delta_f = 0$ ,  $\Phi = \pi/6$ ,  $l = 1$ ,  $\Omega_c = \gamma$ ,  $M = N = R = 4$ ,  $L = 7$ , and  $r/\omega = 1$ .

equation. Further, in Section III we present the numerical outcomes and their analysis under different parameters of the system, e.g., laser field detunings and vorticity of the composite Laguerre-Gaussian beam. In the last section we give a summary of the obtained results and outline possible experimental realizations and applications.

## II. MODEL AND EQUATIONS

We start by considering the four-level  $N$ -type atomic system shown in Fig. 1, which consists of two lower states  $|1\rangle$  and  $|2\rangle$ , and two excited states  $|3\rangle$  and  $|4\rangle$ . A weak probe field with Rabi frequency  $\Omega_p$  interacts with the transition  $|1\rangle \rightarrow |3\rangle$ , while two coupling fields with Rabi frequencies  $\Omega_c$  and  $\Omega_F$  drive the atomic transitions  $|2\rangle \rightarrow |3\rangle$  and  $|2\rangle \rightarrow |4\rangle$ , respectively. The Rabi frequencies of the optical fields are defined as  $\Omega_p = \vec{\mu}_{13} \cdot \vec{E}_p/2\hbar$ ,  $\Omega_c = \vec{\mu}_{23} \cdot \vec{E}_c/2\hbar$ , and  $\Omega_F = \vec{\mu}_{24} \cdot \vec{E}_F/2\hbar$ , where  $\vec{\mu}_{ij}$  represents the electric-dipole matrix element of the transition  $|i\rangle \rightarrow |j\rangle$ .

Next, we proceed to write down the Hamiltonian of the system in the interaction picture under the electric dipole and rotating-wave approximations:

$$H_{\text{int}} = -\hbar(\Delta_p - \Delta_c)|2\rangle\langle 2| - \hbar\Delta_p|3\rangle\langle 3| - \hbar(\Delta_p - \Delta_c + \Delta_f) \\ \times |4\rangle\langle 4| - \hbar(\Omega_p|3\rangle\langle 1| + \Omega_c|3\rangle\langle 2| + \Omega_F|4\rangle\langle 2| + \text{H.c.}). \quad (1)$$

Here, the detunings of the corresponding laser fields are denoted by  $\Delta_p = \omega_p - \omega_{31}$ ,  $\Delta_c = \omega_c - \omega_{32}$ , and  $\Delta_f = \omega_F - \omega_{42}$ , where  $\omega_{ij}$  ( $i, j = 1 \dots 4$ ) is the atomic resonant frequency of the  $|i\rangle \rightarrow |j\rangle$  transition, while  $\omega_p$ ,  $\omega_c$ , and  $\omega_f$  are the laser field frequencies.

The wave function describing the system can be decomposed into the basis set of the unperturbed Hamiltonian  $\{|1\rangle, |2\rangle, |3\rangle, |4\rangle\}$  as  $\Psi(t) = \sum_{i=1,4} a_i(t)e^{-i\omega_i t}|i\rangle$ , where  $a_i(t)$  are the corresponding time-dependent coefficients and  $\hbar\omega_i$  denotes the energy of each unperturbed atomic level  $|i\rangle$ . The system dynamics can then be described by the motion equations for the probability amplitude of all the states involved in the interaction, as follows:

$$\begin{aligned} \dot{a}_1 &= i\Omega_p a_3, \\ \dot{a}_2 &= i[(\Delta_p - \Delta_c)a_2 + \Omega_c a_3 + \Omega_F a_4] - \gamma_2 a_2, \\ \dot{a}_3 &= i(\Omega_p a_1 + \Omega_c a_2 + \Delta_p a_3) - \frac{\Gamma_3}{2} a_3, \\ \dot{a}_4 &= i[\Omega_F a_2 + (\Delta_p - \Delta_c + \Delta_f)a_4] - \frac{\Gamma_4}{2} a_4. \end{aligned} \quad (2)$$

Here  $\Gamma_3$  and  $\Gamma_4$  are the decay rates from the upper atomic levels and  $\gamma_2$  represents the decoherence rate of the ground state. For simplicity, we assume  $\Gamma_3 = \Gamma_4 = \gamma$  and the other parameters take  $\gamma$  as a unit. The atomic-optical response of the probe field is described by the susceptibility  $\chi_p$ . By solving

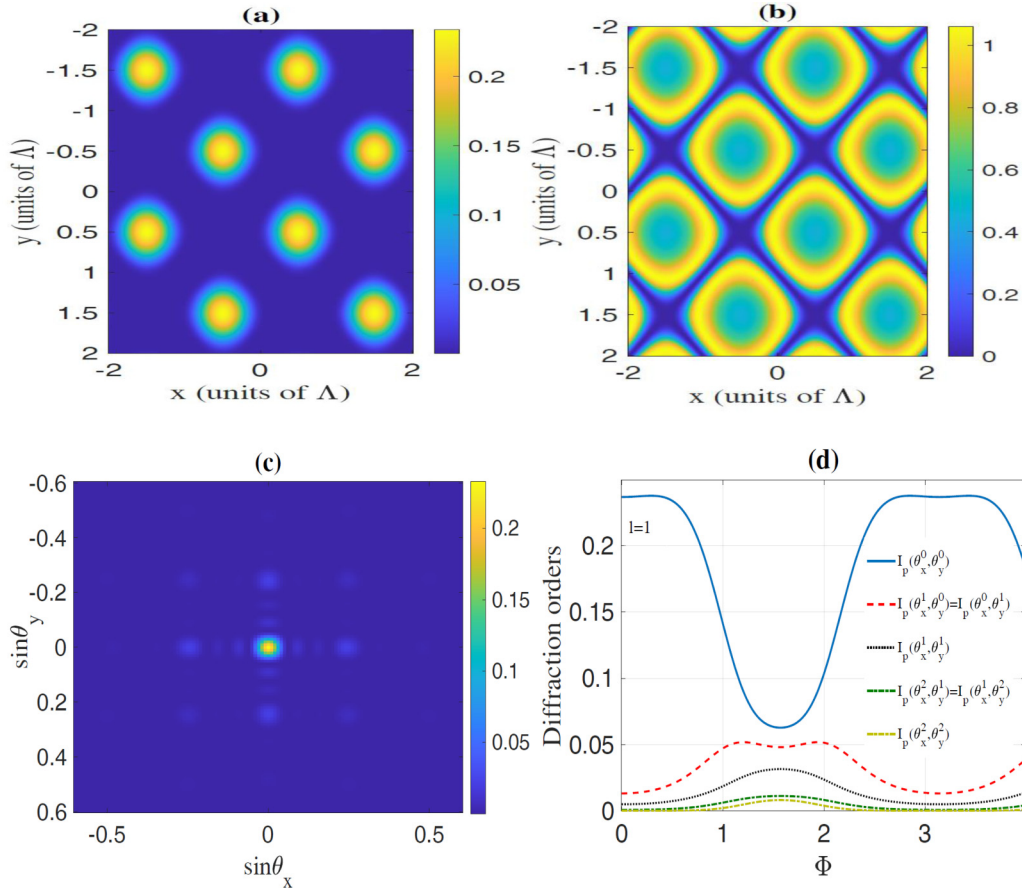


FIG. 4. Amplitude (a) and phase (b) modulations of probe light as function of  $x$ ,  $y$ , and diffraction pattern (c) as a function of  $\sin\theta_x$  and  $\sin\theta_y$ . (d) The diffraction intensities  $I_p(\theta_x^0, \theta_y^0)$ ,  $I_p(\theta_x^1, \theta_y^0)$ ,  $I_p(\theta_x^1, \theta_y^1)$ ,  $I_p(\theta_x^2, \theta_y^1)$ , and  $I_p(\theta_x^2, \theta_y^2)$  as a function of the phase  $\Phi$ . The selected parameters are  $\Delta_p = 0$ ,  $\Delta_c = \Delta_f = \gamma$ ,  $\Phi = \pi/6$ ,  $l = 1$ ,  $\Omega_c = \gamma$ ,  $M = N = R = 4$ ,  $L = 7$ , and  $r/w = 1$ .

Eqs. (2) under the steady-state condition and the weak probe field approximation (which implies that  $|a_1|^2 \approx 1$ ), as well as using the polarization of the medium  $\vec{P}_p = N\mu_{13}^* a_3 a_1^*$ , the susceptibility of the probe field can be written as

$$\chi_p = \frac{N\mu_{13}^2}{2\varepsilon_0\hbar} \chi. \quad (3)$$

In the above equation,  $N$  denotes the atomic density,  $\varepsilon_0$  is the dielectric constant in vacuum, and  $\chi$  is given by the expression

$$\chi = \frac{A_2 A_4 - \Omega_F^2}{A_4(A_2 A_3 - \Omega_c^2) - A_3 \Omega_F^2}, \quad (4)$$

with  $A_2 = \Delta_p - \Delta_c + i\gamma_2$ ,  $A_3 = \Delta_p + i\frac{\Gamma_3}{2}$ , and  $A_4 = \Delta_p - \Delta_c + \Delta_f + i\frac{\Gamma_4}{2}$ .

As is well known, due to the intensity-dependent susceptibility, control fields with standing-wave patterns lead to spatially modulated absorption and refraction for the probe field. Thus, the atoms act as a grating which can diffract the probe beam into different directions.

To this end, in our model we will replace the coupling field  $\Omega_c$  by a SW in two directions, i.e.,  $\Omega[\sin(\pi x/\Lambda_x) + \sin(\pi y/\Lambda_y)]$ , with  $\Lambda_x$  and  $\Lambda_y$  being the space frequencies of the SW. The coupling Rabi frequency  $\Omega_F$  is assumed to be a

composite vortex beam of the form

$$\Omega_F = \Omega e^{-r^2/w^2} [(r/w)^{|l_1|} e^{il_1\Phi} + (r/w)^{|l_2|} e^{il_2\Phi}], \quad (5)$$

which is a superposition of two vortex fields. Here  $r = \sqrt{x^2 + y^2}$  stands for the radial distance from the axis of the Laguerre-Gaussian (LG) beam, while  $\Phi$ ,  $l$ , and  $w$  are the azimuthal angle, the vorticity, and the beam waist parameter, respectively. Assuming that  $l_1 = -l_2 = l$ , one can write  $\Omega_F = \Omega_f \cos(l\Phi)$ , where  $\Omega_f = 2\Omega e^{-r^2/w^2} (r/w)^{|l|}$ . Clearly, the susceptibility of the medium given by Eq. (4) depends on the OAM number of the composite beam. It is worth noting, that while the usual LG beams are not periodic, the coaxial superposition of two or more LG beams of different azimuthal indices create composite vortex beams with shifted axes. When  $l_1 < l_2 = l$ , the resulting composite twisted beam contains a vortex of charge  $l_1$  located at the beam center which is surrounded by  $l_1 - l_2$  peripheral vortices. The case of  $l_1 = -l_2 = l$  and equal intensities, leads to the  $2\cos(l\Phi)$  azimuthal dependence of the composite field. The latter corresponds to the flowerlike periodic ‘‘petals’’ intensity structures [40,47].

The diffraction pattern of the probe light through the medium can be obtained by using the Maxwell’s equation under the slowly varying envelope approximation in steady-state

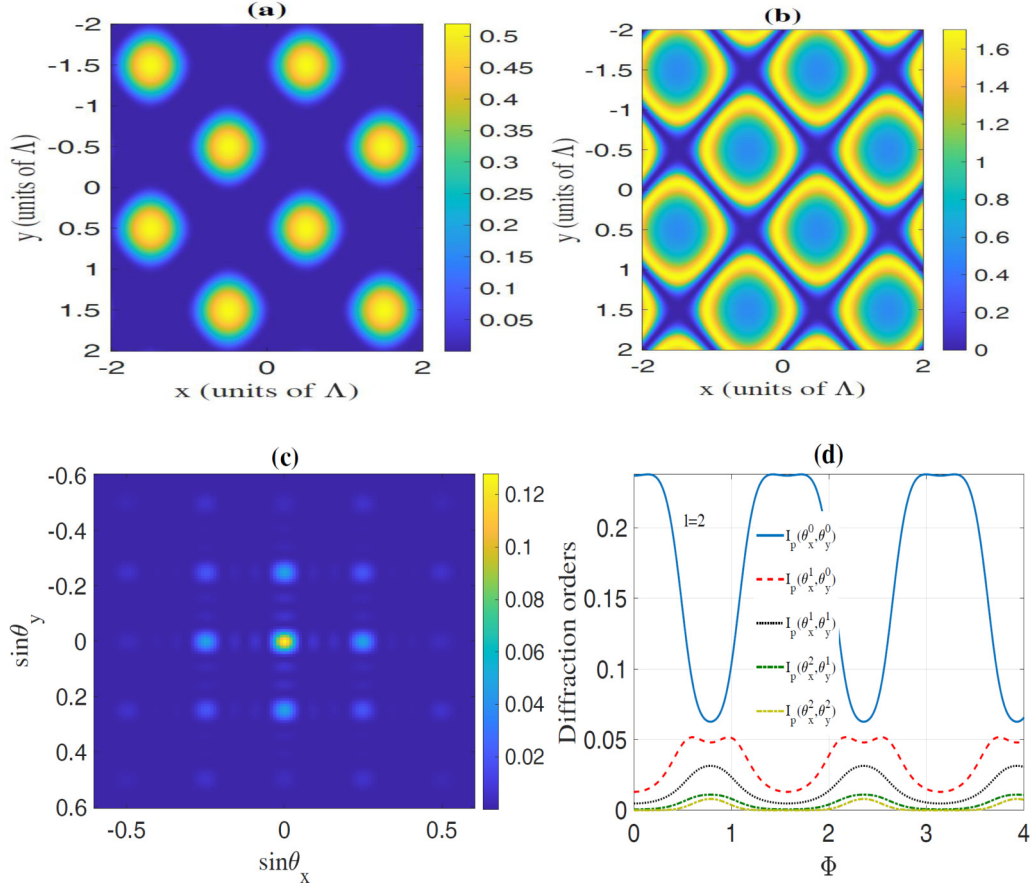


FIG. 5. Amplitude (a) and phase (b) modulations of probe light as a function of  $x, y$  and diffraction pattern (c) as a function of  $\sin \theta_x$  and  $\sin \theta_y$ . (d) The diffraction intensities  $I_p(\theta_x^0, \theta_y^0)$ ,  $I_p(\theta_x^1, \theta_y^0)$ ,  $I_p(\theta_x^1, \theta_y^1)$ ,  $I_p(\theta_x^2, \theta_y^1)$ , and  $I_p(\theta_x^2, \theta_y^2)$  as a function of the phase  $\Phi$ . The selected parameters are  $\Delta_p = 0$ ,  $\Delta_c = \Delta_f = \gamma$ ,  $\Phi = \pi/6$ ,  $l = 2$ ,  $\Omega_c = \gamma$ ,  $M = N = R = 4$ ,  $L = 7$ , and  $r/w = 1$ .

regime:

$$\frac{\partial E_p}{\partial z} = i \frac{\pi}{\varepsilon_0 \lambda_p} P_p, \quad P_p = \varepsilon_0 \chi(\omega_p) E_p, \quad (6)$$

where the parameter  $\lambda_p$  corresponds to the wavelength of the probe light.

Then, the transmission function for an interaction length  $L$  of the two-dimensional grating is given by

$$T(x, y) = e^{-\text{Im}[\chi(\omega_p)]L} e^{i\text{Re}[\chi(\omega_p)]L} = e^{-\alpha(x,y)} e^{i\varphi(x,y)L}. \quad (7)$$

The first term in the exponent denotes the grating amplitude and the second term corresponds to the phase modulation. By using the Fourier transformation of the transmission function  $T(x, y)$  we obtain the Fraunhofer diffraction equation as follows:

$$I_p(\theta_x, \theta_y) = |E(\theta_x, \theta_y)|^2 \times \frac{\sin^2(M\pi \Lambda_x \sin \theta_x / \lambda_p) \sin^2(N\pi \Lambda_y \sin \theta_y / \lambda_p)}{M^2 N^2 \sin^2(\pi \Lambda_x \sin \theta_x / \lambda_p) \sin^2(\pi \Lambda_y \sin \theta_y / \lambda_p)}. \quad (8)$$

Here we have

$$E(\theta_x, \theta_y) = \int_0^1 T(x, y) \exp(-i2\pi x \Lambda_x \sin \theta_x / \lambda_p) \times \exp(-i2\pi y \Lambda_y \sin \theta_y / \lambda_p) dx dy, \quad (9)$$

where  $\theta_x$  and  $\theta_y$  stand for the diffraction angles with respect to the  $z$  direction. The  $(m, n)$ th order diffraction angle is determined by the grating equations  $\sin \theta_x = m\lambda_p / \Lambda_x$  and  $\sin \theta_y = n\lambda_p / \Lambda_y$ , where  $m$  and  $n$  are the spatial period numbers of the atomic grating. We can further obtain the diffraction intensities of the  $(m, n)$  orders as follows:

$$I(\theta_x^m, \theta_y^n) = \left| \int_0^1 T(x, y) e^{-i2\pi mx} e^{-i2\pi ny} dx dy \right|^2. \quad (10)$$

### III. RESULTS AND DISCUSSION

In this section, we will analyze the effects which the different system parameters play on the amplitude and phase modulation, as well as the controllability of the diffraction intensity of the probe field across the four-level  $N$ -type atomic system. We also investigate the effects of the orbital angular momentum parameter  $l$  on the properties and diffraction power of the grating.

#### A. Vortex field Rabi frequencies

In Fig. 2, we display the magnitude of the Rabi frequencies  $\Omega_f$  (a) and  $\Omega_F$  (b) versus  $r/w$  for a value of  $\Phi = \pi/6$  when the OAM number of the composite vortex light is changed. From Fig. 2(a) one finds that when  $r = w$  the Rabi frequency  $\Omega_f$  is identical for all values of the OAM number. However,

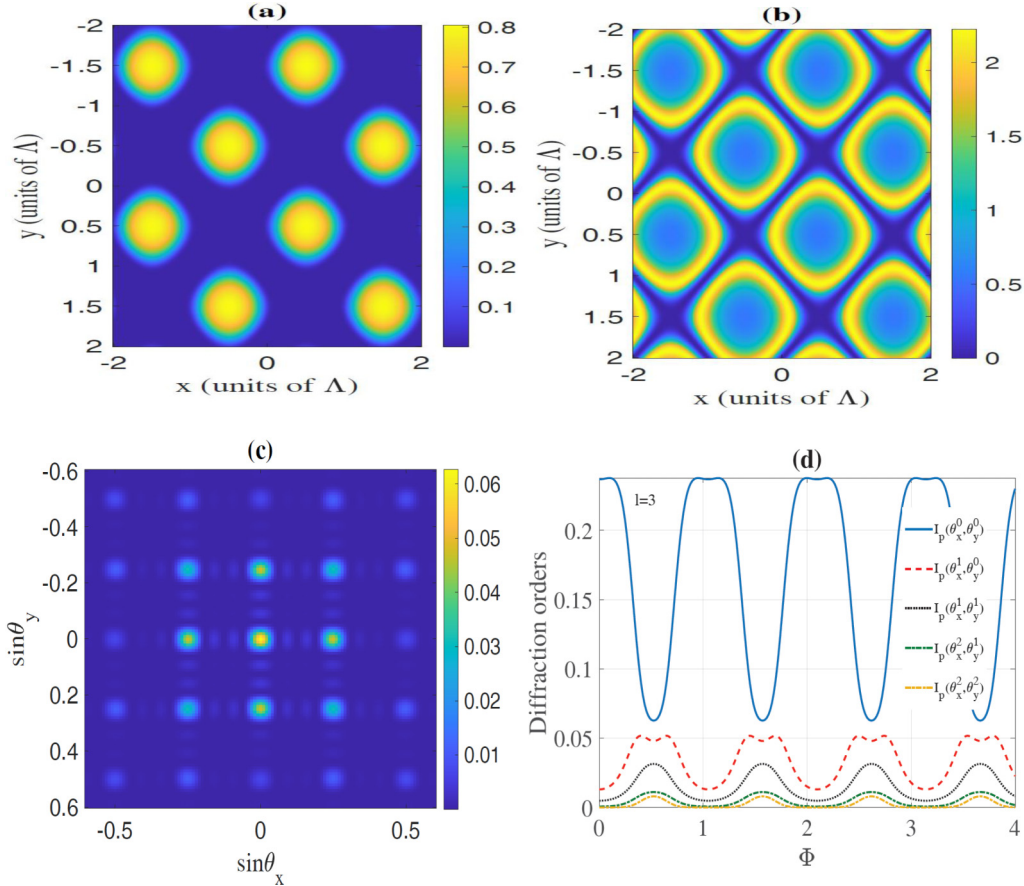


FIG. 6. Amplitude (a) and phase (b) modulations of probe light as a function of  $x$ ,  $y$ , and diffraction pattern (c) as a function of  $\sin \theta_x$  and  $\sin \theta_y$ . (d) The diffraction intensities  $I_p(\theta_x^0, \theta_y^0)$ ,  $I_p(\theta_x^1, \theta_y^0)$ ,  $I_p(\theta_x^1, \theta_y^1)$ ,  $I_p(\theta_x^2, \theta_y^1)$ , and  $I_p(\theta_x^2, \theta_y^2)$  as a function of the phase  $\Phi$ . The selected parameters are  $\Delta_p = 0$ ,  $\Delta_c = \Delta_f = \gamma$ ,  $\Phi = \pi/6$ ,  $l = 3$ ,  $\Omega_c = \gamma$ ,  $M = N = R = 4$ ,  $L = 7$ , and  $r/w = 1$ .

Fig. 2(b) shows that the value of  $\Omega_F$  is changed when we alter the value of  $l$ . The Rabi frequency of the coupling light is strong when  $l = 1$  and completely vanishes for a value of  $l = 3$ . In the latter case ( $l = 3$ ) the four-level  $N$ -type medium converts to the three-level  $\Lambda$ -type system.

### B. Resonant probe and coupling fields

Next, we will investigate the effects of different probe and coupling field detunings. In Fig. 3 we plot the dependence of the amplitude modulation (a), phase modulation (b), Fraunhofer diffraction (c), and different diffraction orders (d) of the probe light under resonance condition of all the applied fields for an OAM number  $l = 1$ . We realize that the amplitude modulation of the probe field (a) is more pronounced than its phase modulation (b). In fact, the phase modulation has a zero value, meaning that in this case we can achieve only an amplitude grating, as depicted in Fig. 3(c). The main energy of the probe light is gathered in the zero order, while the high orders of diffraction completely disappear. In Fig. 3(d) we display the different orders of diffraction  $I_p(\theta_x^i, \theta_y^j)$  versus the azimuthal angle of the composite vortex light. The figure confirms our previous observation, that most of the probe energy remains in the zero order and the high orders have zero values.

### C. Resonant probe and off-resonant coupling fields

As a next step, in Fig. 4 we study the situation when the standing wave and the composite vortex light are off-resonant with their transitions, while the probe field remains resonant. In this case, we find that the amplitude (a) and phase (b) modulations of the probe light become nonzero; however, their values are small.

The main energy of the probe light gathers in the zero order, while the diffraction into high orders is very weak (c). From Fig. 4(d), we conclude that the different orders of diffraction are altered when the azimuthal angle of the composite vortex light changes. For each value of the azimuthal angle of the composite vortex light most of the probe energy remains in the zero order  $I_p(\theta_x^0, \theta_y^0)$ . However, for some special cases, such as  $\Phi = \pi/2$ , the difference between the intensities of the zero and high orders is low. When  $l = 1$  and  $\Phi = \pi/2$  the intensity of the composite vortex light becomes zero, therefore the four-level  $N$ -type atomic system converts to the three-level atomic system. In this case, the absorption and dispersion of the probe light may be significantly manipulated. As a result, some of the probe energy may transfer from zero order to high order of grating.

Further, we will investigate the behavior of the grating upon alternating the vortex number  $l$  of the Laguerre-Gaussian field. Figures 5 and 6 show the dependence of the

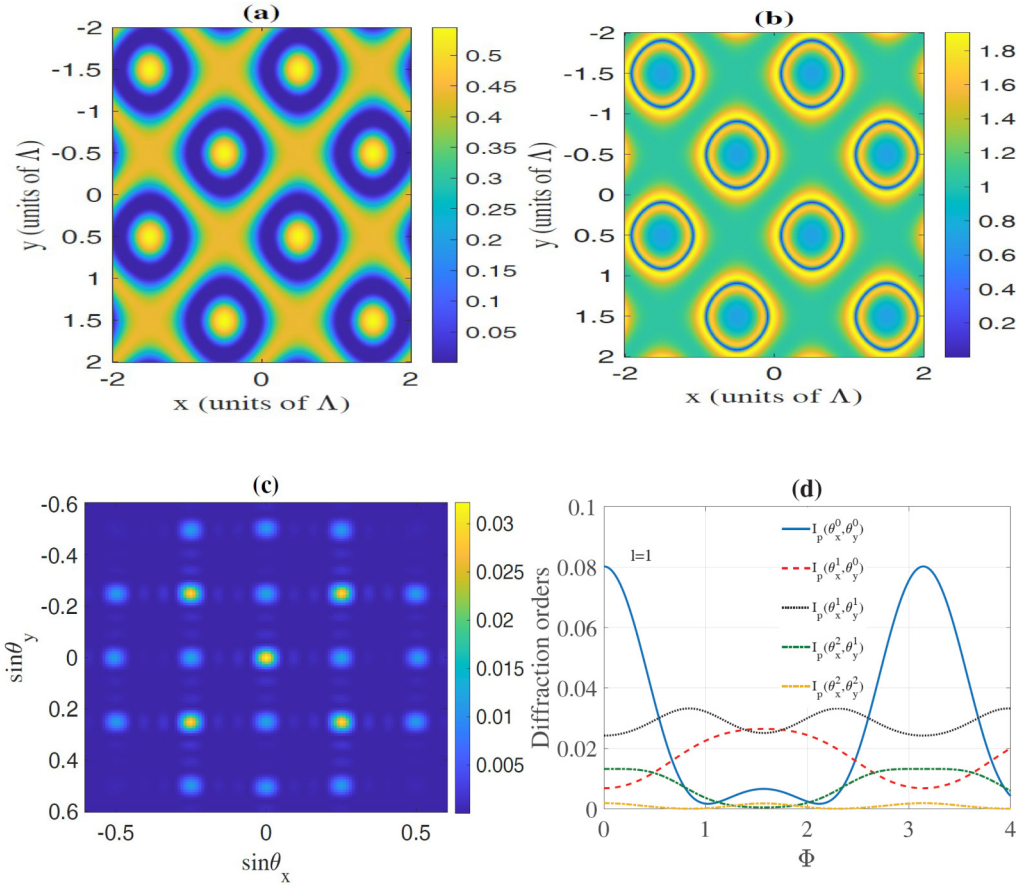


FIG. 7. Amplitude (a) and phase (b) modulations of probe light as a function of  $x, y$ , and diffraction pattern (c) as a function of  $\sin\theta_x$  and  $\sin\theta_y$ . (d) The diffraction intensities  $I_p(\theta_x^0, \theta_y^0)$ ,  $I_p(\theta_x^1, \theta_y^0)$ ,  $I_p(\theta_x^1, \theta_y^1)$ ,  $I_p(\theta_x^2, \theta_y^1)$ , and  $I_p(\theta_x^2, \theta_y^2)$  as a function of the phase  $\Phi$ . The selected parameters are  $\Delta_p = 2\gamma$ ,  $\Delta_c = \Delta_f = \gamma$ ,  $\Phi = \pi/6$ ,  $l = 1$ ,  $\Omega_c = \gamma$ ,  $M = N = R = 4$ ,  $L = 7$ , and  $r/w = 1$ .

amplitude modulation (a), phase modulation (b), Fraunhofer diffraction (c), and different diffraction orders (d) of the probe light on the values of the OAM number  $l = 2, 3$ . We realize that the amplitude and phase modulations of the probe field are enhanced when we change  $l$  to 2 and 3. For  $l = 2$  the main energy of the probe light gathers in the zero order and only a small portion of the probe energy transfers to the high orders. As  $l$  increases to 3, some of the probe energy may transfer to the high orders of the grating; however, the intensity of the zero order still remains higher than that of the high orders.

#### D. Off-resonant probe and coupling fields

As a next step, we will study the effects of the OAM number in the case when all of the applied fields are off-resonant with their transitions, e.g.,  $\Delta_p = 2\gamma$  and  $\Delta_c = \Delta_f = \gamma$ .

In Figs. 7–9 are shown the behaviors of the amplitude modulation (a), phase modulation (b), Fraunhofer diffraction (c), and different diffraction orders (d) of the probe light for OAM numbers  $l = 1, 2, 3$ . We observe that the amplitude modulation of the probe light [Figs. 7(a)–9(a)] decreases when we change the OAM number from  $l = 1$  to  $l = 3$ . At the same time, the phase modulation of the probe light [Figs. 7(b)–9(b)] increases by enhancing the  $l$  number, which causes a

probe energy transfer from the zero to the high orders of the grating. Some of the probe energy transfers to the second order of diffraction, with their intensities being weaker than those of the first order of diffraction. The variation of the different order of diffraction versus the azimuthal angle [Figs. 7(d)–9(d)], show that by adjusting the amplitude and phase modulations, more of the probe energy transfers to the high order directions, which improves the diffracted power. We find that the main part of the probe energy transfer occurs to  $I_p(\theta_x^1, \theta_y^1)$  and  $I_p(\theta_x^1, \theta_y^0)$ . This gives us reasons to claim, that by adjusting the azimuthal angle of the composite vortex light one can control the intensities of the different orders. Since in most previous works the transfer of probe energy is reported from the zero order to the first order of the grating, we are specifically interested in investigating the opportunities for transferring probe energy to the second and higher orders. In Fig. 10 we present the Fraunhofer diffraction (a) and the different orders of diffraction (b) versus the parameter  $r/w$  of the composite vortex field. We find that for  $\Phi = \pi/4$  and  $l = 1$ , most of the probe energy transfers to the first order and some of the probe energy transfers to the second order of the grating. Therefore, in this case the probe energy is mainly shifted into the (1, 1) and (2, 2) order of the diffraction peaks and the diffraction efficiency of the created grating is improved.

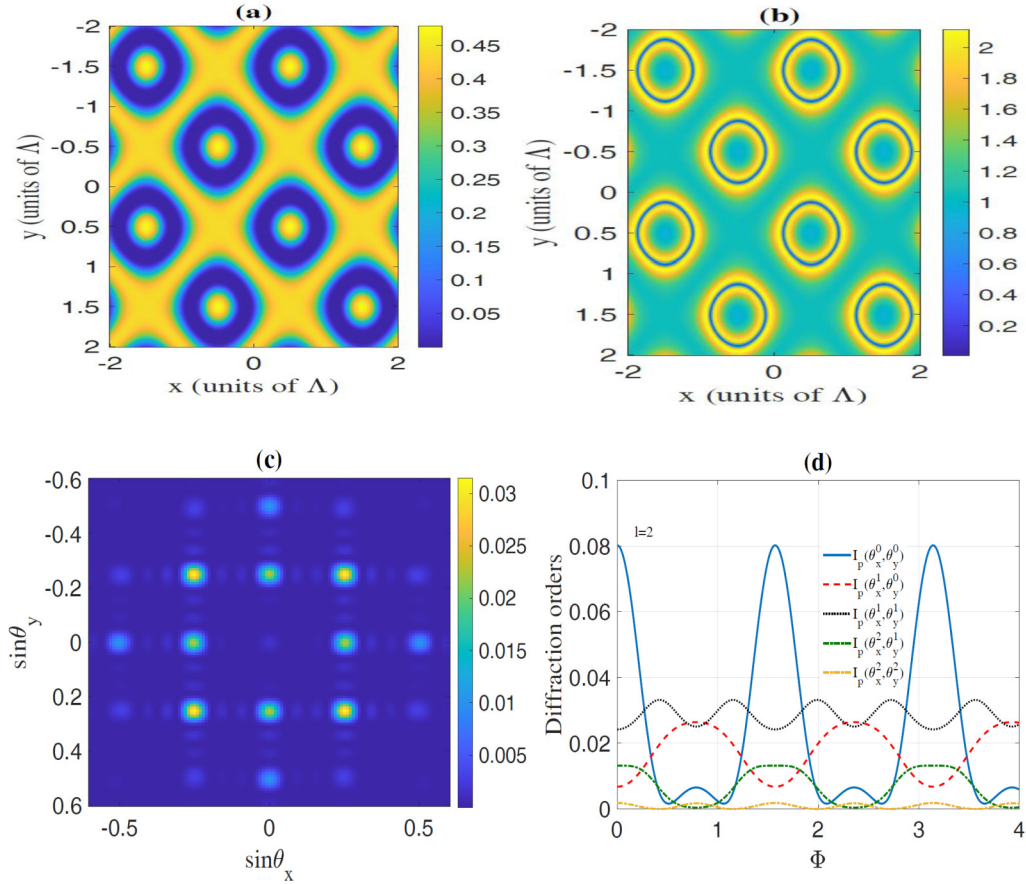


FIG. 8. Amplitude (a) and phase (b) modulations of probe light as a function of  $x, y$ , and diffraction pattern (c) as a function of  $\sin\theta_x$  and  $\sin\theta_y$ . (d) The diffraction intensities  $I_p(\theta_x^0, \theta_y^0)$ ,  $I_p(\theta_x^1, \theta_y^0)$ ,  $I_p(\theta_x^1, \theta_y^1)$ ,  $I_p(\theta_x^2, \theta_y^1)$ , and  $I_p(\theta_x^2, \theta_y^2)$  as a function of the phase  $\Phi$ . The selected parameters are  $\Delta_p = 2\gamma$ ,  $\Delta_c = \Delta_f = \gamma$ ,  $\Phi = \pi/6$ ,  $l = 2$ ,  $\Omega_c = \gamma$ ,  $M = N = R = 4$ ,  $L = 7$ , and  $r/w = 1$ .

#### IV. CONCLUSIONS

In this work we investigated the performance of a two-dimensional EIG created upon the simultaneous coupling of an atomic  $N$ -type excitation scheme by a standing-wave field along the  $x, y$  direction and a composite vortex field. Numerical analysis of the behavior of the amplitude modulations, phase modulations, and the different order diffraction intensities of the probe field, show that the produced grating is symmetric for different probe and coupling field detunings, as well as orbital angular momenta of the Laguerre-Gaussian beam. The variation of the azimuthal number serves as an easy control knob for achieving direct control over the distribution of the diffraction intensities, and thus, on the performance of the proposed grating. This additional degree of freedom, originating from the utilization of the composite optical vortex field, allows us to exceed the opportunities provided by previously studied EIGs. Compared to previous studies, where different mechanisms (SGC, relative phase between the applied lights) have been used for transferring the probe energy from zero order to high orders, our proposed model is advantageous by providing an easy way for controlling the phase grating mechanism only via adjusting the OAM number and the azimuthal angle of the composite vortex light. Because of

this easily achievable controllability, we envisage a feasible experimental realization of the proposed grating scheme in typical atomic EIG setups. The latter opens up the possibility for novel applications in all-optical information processing and atom-manipulation technologies, in view of providing an additional level of flexibility to all-optical quantum switches, logic gates, and other EIT-based devices. It is interesting to note, that since both the two-dimensional standing wave and the Laguerre-Gaussian beam are symmetric, in the scheme proposed here we obtain a symmetric grating. Alternatively, in our recent article [54] we have shown that an asymmetric grating pattern is observed when applying asymmetric coupling light. To this end, as a future work we plan to address the question of  $\mathcal{PT}$ -symmetric quantum systems interacting with composite vortex light.

#### ACKNOWLEDGMENTS

This work was supported by a STSM from COST Action CA16221 for T.K. and H.R.H. S.H.A. would like to thank the Iran National Science Foundation (INSF) and Research deputy of Iran University of Science and Technology (Grant No. 98017089).



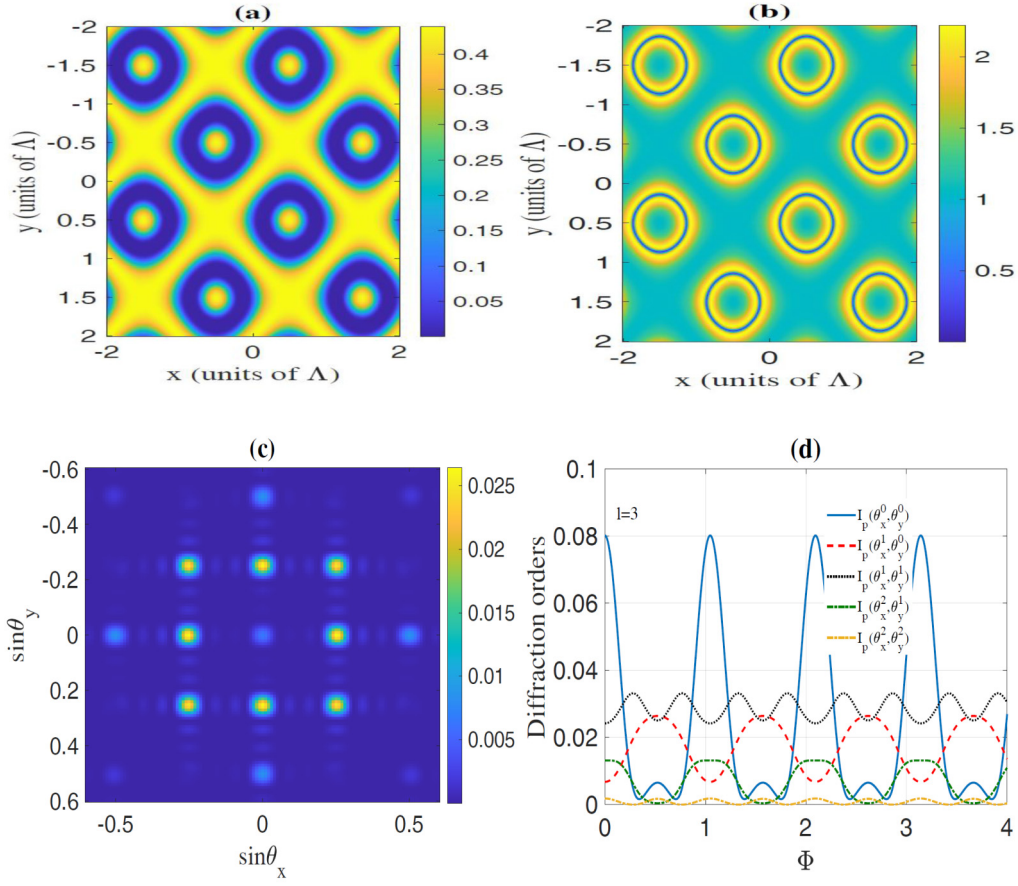


FIG. 9. Amplitude (a) and phase (b) modulations of probe light as a function of  $x$ ,  $y$ , and diffraction pattern (c) as a function of  $\sin \theta_x$  and  $\sin \theta_y$ . (d) The diffraction intensities  $I_p(\theta_x^0, \theta_y^0)$ ,  $I_p(\theta_x^1, \theta_y^0)$ ,  $I_p(\theta_x^1, \theta_y^1)$ ,  $I_p(\theta_x^2, \theta_y^1)$ , and  $I_p(\theta_x^2, \theta_y^2)$  as a function of the phase  $\Phi$ . The selected parameters are  $\Delta_p = 2\gamma$ ,  $\Delta_c = \Delta_f = \gamma$ ,  $\Phi = \pi/6$ ,  $l = 3$ ,  $\Omega_c = \gamma$ ,  $M = N = R = 4$ ,  $L = 7$ , and  $r/w = 1$ .

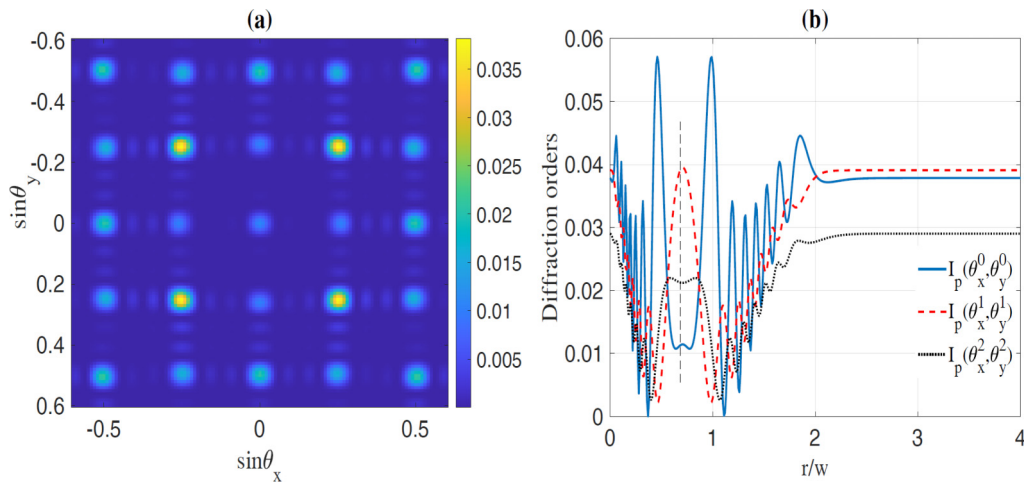


FIG. 10. (a) The diffraction pattern as a function of  $\sin \theta_x$  and  $\sin \theta_y$ . (b) The diffraction intensities  $I_p(\theta_x^0, \theta_y^0)$ ,  $I_p(\theta_x^1, \theta_y^1)$ , and  $I_p(\theta_x^2, \theta_y^2)$  as a function of  $r/w = 1$ . The selected parameters are  $\Phi = \pi/4$ ,  $l = 1$ , and  $\Delta_f = -\gamma$ . Other parameters are the same as in Fig. 9.

- [1] S. E. Harris, Electromagnetically induced transparency, *Phys. Today* **50** (7), 36 (1997).
- [2] M. Fleischhauer, A. Imamoglu, and J. P. Marangos, Electromagnetically induced transparency: Optics in coherent media, *Rev. Mod. Phys.* **77**, 633 (2005).
- [3] A. V. Turukhin, V. S. Sudarshanam, M. S. Shahriar, J. A. Musser, B. S. Ham, and P. R. Hemmer, Observation of Ultraslow and Stored Light Pulses in a Solid, *Phys. Rev. Lett.* **88**, 023602 (2001).
- [4] J. Marangos, Slow light in cool atoms, *Nature (London)* **397**, 559 (1999).
- [5] D. F. Phillips, A. Fleischhauer, A. Mair, R. L. Walsworth, and M. D. Lukin, Storage of Light in Atomic Vapor, *Phys. Rev. Lett.* **86**, 783 (2001).
- [6] M. Johnsson and K. Mølmer, Storing quantum information in a solid using dark-state polaritons, *Phys. Rev. A* **70**, 032320 (2004).
- [7] M. D. Lukin and A. Imamoglu, Controlling photons using electromagnetically induced transparency, *Nature (London)* **413**, 273 (2001).
- [8] S. E. Harris, J. E. Field, and A. Imamoglu, Nonlinear Optical Processes Using Electromagnetically Induced Transparency, *Phys. Rev. Lett.* **64**, 1107 (1990).
- [9] M. D. Lukin and A. Imamoglu, Nonlinear Optics and Quantum Entanglement of Ultraslow Single Photons, *Phys. Rev. Lett.* **84**, 1419 (2000).
- [10] H. Y. Ling, Y. Q. Li, and M. Xiao, Electromagnetically induced grating: Homogeneously broadened medium, *Phys. Rev. A* **57**, 1338 (1998).
- [11] M. Mitsunaga and N. Imoto, Observation of an electromagnetically induced grating in cold sodium atoms, *Phys. Rev. A* **59**, 4773 (1999).
- [12] G. S. Cardoso and J. W. R. Tabosa, Electromagnetically induced gratings in a degenerate open two-level system, *Phys. Rev. A* **65**, 033803 (2002).
- [13] A. W. Brown and M. Xiao, All-optical switching and routing based on an electromagnetically induced absorption grating, *Opt. Lett.* **30**, 699 (2005).
- [14] D. Moretti, D. Felinto, J. Tabosa, and A. Lezama, Dynamics of a stored Zeeman coherence grating in an external magnetic field, *J. Phys. B: At., Mol. Opt. Phys.* **43**, 115502 (2010).
- [15] L. Zhao, W. Duan, and S. F. Yelin, All-optical beam control with high speed using image-induced blazed gratings in coherent media, *Phys. Rev. A* **82**, 013809 (2010).
- [16] H. Zhang, J. Yuan, S. Dong, C. Wu, and L. Wang, Observation of an electromagnetically induced grating in cold  $^{85}\text{Rb}$  atoms, *Appl. Sci.* **10**, 5740 (2020).
- [17] B. K. Dutta and P. K. Mahapatra, Electromagnetically induced grating in a three-level  $\xi$ -type system driven by a strong standing wave pump and weak probe fields, *J. Phys. B: At., Mol. Opt. Phys.* **39**, 1145 (2006).
- [18] T. Naseri and R. Sadighi-Bonabi, Electromagnetically induced phase grating via population trapping condition in a microwave-driven four-level atomic system, *J. Opt. Soc. Am. B* **31**, 2879 (2014).
- [19] L. Wang, F. Zhou, P. Hu, Y. Niu, and S. Gong, Two dimensional electromagnetically induced cross-grating in a four-level tripod-type atomic system, *J. Phys. B: At., Mol. Opt. Phys.* **47**, 225501 (2014).
- [20] M. Sahrai, F. Bozorgzadeh, and H. Khoshshima, Phase control of electromagnetically induced grating in a four-level atomic system, *Opt. Quant. Electron.* **48**, 438 (2016).
- [21] S. Hossein Asadpour, A. Panahpour, and M. Jafari, Phase dependent electromagnetically induced grating in a four level quantum system near a plasmonic nanostructure, *Eur. Phys. J. Plus* **133**, 411 (2018).
- [22] S.-C. Tian, R.-G. Wan, L.-J. Wan, Sh.-L. Shu, H.-Y. Lu, X. Zhan, C.-Z. Tong, J.-L. Feng, M. Xiao, and L.-J. Wang, Asymmetric light diffraction of two dimensional electromagnetically induced grating with  $PT$  symmetry in asymmetric double quantum wells, *Opt. Express* **26**, 32918 (2018).
- [23] F. Wen, W. Wang, I. Ahmed, H. Wang, Y. Zhang, Y. Zhang, A. R. Mahesar, and M. Xiao, Two-dimensional Talbot self-imaging via electromagnetically induced lattice, *Sci. Rep.* **7**, 41790 (2017).
- [24] S.-q. Kuang, R.-g. Wan, J. Kou, Y. Jiang, and J. Gao, Tunable double photonic bandgaps in a homogeneous atomic medium, *J. Opt. Soc. Am. B* **27**, 1518 (2010).
- [25] P. W. Zhai, X. M. Su, and J. Y. Gao, Optical bistability in electromagnetically induced grating, *Phys. Lett. A* **289**, 27 (2001).
- [26] Y. Zhang, C. Yuan, Y. Zhang, H. Zheng, H. Chen, C. Li, Z. Wang, and M. Xiao, Surface solitons of four-wave mixing in an electromagnetically induced lattice, *Laser Phys. Lett.* **10**, 055406 (2013).
- [27] Y. Zhang, Z. Wang, Z. Nie, C. Li, H. Chen, K. Lu, and M. Xiao, Four-Wave Mixing Dipole Soliton in Laser-Induced Atomic Gratings, *Phys. Rev. Lett.* **106**, 093904 (2011).
- [28] F. Gao, Y. M. Liu, X. D. Tian, C. L. Cui, and J. H. Wu, Intrinsic link of asymmetric reflection and diffraction in non-Hermitian gratings, *Opt. Express* **26**, 33818 (2018).
- [29] A. A. Naeimi, E. Darabi, A. Mortezaipoor, and G. Naemi, Phase-controlled optical  $PT$  symmetry and asymmetric light diffraction in one- and two-dimensional optical lattices, *Eur. Phys. J. Plus* **135**, 791 (2020).
- [30] M. Abbas, A. Khurshid, I. Hussain, and A. N. D. Ziauddin, Investigation of  $PT$ - and  $PT$ -antisymmetry in two dimensional (2D) optical lattices, *Opt. Express* **28**, 8003 (2020).
- [31] D. L. Andrews and M. Babiker, *The Angular Momentum of Light* (Cambridge University Press, Cambridge, UK, 2012).
- [32] J. Wang, Advances in communications using optical vortices, *Opt. Express* **5**, B14 (2016).
- [33] J. Wang, J. Y. Yang, I. M. Fazal, N. Ahmed, Y. Yan, H. Huang, Y. Ren, Y. Yue, S. Dolinar, M. Tur, and A. E. Willner, Terabit free-space data transmission employing orbital angular momentum multiplexing, *Nat. Photonics* **6**, 488 (2012).
- [34] G. Molina-Terriza, J. P. Torres, and L. Torner, Twisted photons, *Nat. Phys.* **3**, 305 (2007).
- [35] S. Sharma and T. N. Dey, Phase-induced transparency mediated structured-beam generation in a closed-loop tripod configuration, *Phys. Rev. A* **96**, 033811 (2017).
- [36] H. R. Hamed, V. Kudriašov, J. Ruseckas, and G. Juzeliūnas, Azimuthal modulation of electromagnetically induced transparency using structured light, *Opt. Express* **26**, 28249 (2018).

- [37] Z. Dutton and J. Ruostekoski, Transfer and Storage of Vortex States in Light and Matter Waves, *Phys. Rev. Lett.* **93**, 193602 (2004).
- [38] J. Ruseckas, G. Juzeliūnas, P. Öhberg, and S. M. Barnett, Polarization rotation of slow light with orbital angular momentum in ultracold atomic gases, *Phys. Rev. A* **76**, 053822 (2007).
- [39] H. R. Hamed, J. Ruseckas, E. Paspalakis, and G. Juzeliūnas, Transfer of optical vortices in coherently prepared media, *Phys. Rev. A* **99**, 033812 (2019).
- [40] H. R. Hamed, E. Paspalakis, G. Zlabys, G. Juzeliūnas, and J. Ruseckas, Complete energy conversion between light beams carrying orbital angular momentum using coherent population trapping for a coherently driven double-lambda atom-light-coupling scheme, *Phys. Rev. A* **100**, 023811 (2019).
- [41] M. Mahdavi, Z. A. Sabegh, M. Mohammadi, M. Mahmoudi, and H. R. Hamed, Manipulation and exchange of light with orbital angular momentum in quantum-dot molecules, *Phys. Rev. A* **101**, 063811 (2020).
- [42] Z. Wang, Y. Zhang, E. Paspalakis, and B. Yu, Efficient spatiotemporal-vortex four-wave mixing in a semiconductor nanostructure, *Phys. Rev. A* **102**, 063509 (2020).
- [43] T. Omatsu, K. Miyamoto, and R. Morita, Optical Vortices Illumination Enables the Creation of Chiral Nanostructures, *Vortex Dynamics and Optical Vortices*, edited by H. Perez-De-Tejada (IntechOpen, Rijeka, 2016), p. 107.
- [44] Q. Zhan, Trapping metallic Rayleigh particles with radial polarization, *Opt. Express* **12**, 3377 (2004).
- [45] M. J. Padgett and R. Bowman, Tweezers with a twist, *Nat. Photonics* **5**, 343 (2011).
- [46] D. Maleev and G. Swartzlander, Composite optical vortices, *J. Opt. Soc. Am. B* **20**, 1169 (2003).
- [47] S. M. Baumann, D. M. Kalb, L. H. MacMillan, and E. J. Galvez, Propagation dynamics of optical vortices due to Gouy phase, *Opt. Express* **17**, 9818 (2009).
- [48] S. Franke-Arnold, J. Leach, M. J. Padgett, V. E. Lembessis, D. Ellinas, A. J. Wright, J. M. Girkin, P. Öhberg, and A. S. Arnold, Optical ferris wheel for ultracold atoms, *Opt. Express* **15**, 8619 (2007).
- [49] X. He, P. Xu, J. Wang, and M. Zhan, Rotating single atoms in a ring lattice generated by a spatial light modulator, *Opt. Express* **17**, 21007 (2009).
- [50] P. Vaity and R. P. Singh, Self-healing property of optical ring lattice, *Opt. Lett.* **36**, 2994 (2011).
- [51] V. E. Lembessis, A. Alqarni, S. Alshamari, A. Siddig, and O. M. Aldossary, Artificial gauge magnetic and electric fields for free two-level atoms interacting with optical ferris wheel light fields, *J. Opt. Soc. Am. B* **34**, 1122 (2017).
- [52] A. S. Desyatnikov, A. A. Sukhorukov, and Y. S. Kivshar, Azimuthons: Spatially Modulated Vortex Solitons, *Phys. Rev. Lett.* **95**, 203904 (2005).
- [53] A. Bekshaev and M. Soskin, Rotational transformations and transverse energy flow in paraxial light beams: Linear azimuthons, *Opt. Lett.* **31**, 2199 (2006).
- [54] S. H. Asadpour, T. Kirova, J. Qia, H. R. Hamed, G. Juzeliūnas, and E. Paspalakis, Azimuthal modulation of electromagnetically induced grating using structured light, *Sci. Rep.* **11**, 20721 (2021).